

## Exploring the Molecular Basis of Action of the Passive Antiglucocorticoid 21-Hydroxy-6,19-epoxyprogesterone

Lautaro D. Álvarez,<sup>†</sup> Marcelo A. Martí,<sup>‡</sup> Adriana S. Veleiro,<sup>†</sup> Diego M. Presman,<sup>§</sup> Darío A. Estrin,<sup>‡</sup> Adalí Pecci,<sup>§</sup> and Gerardo Burton<sup>\*†</sup>

*Departamento de Química Orgánica/UMYFOR-CONICET, Departamento de Química Inorgánica, Analítica y Química Física/INQUIMAE-CONICET, and Departamento de Química Biológica/IFIBYNE-CONICET, Facultad de Ciencias Exactas y Naturales, Universidad de Buenos Aires, Ciudad Universitaria, Pabellón 2, Buenos Aires C1428EGA, Argentina*

Received September 8, 2007

21-Hydroxy-6,19-epoxyprogesterone (21OH-6,19OP) is a selective antiglucocorticoid that lacks the bulky substituent at C-11 found in active antagonists of the glucocorticoid receptor (GR). Ligand-free GR ligand-binding domain (LBD) and GR LBD complexed with 21OH-6,19OP or the agonist dexamethasone were simulated during 6 ns using molecular dynamics. Results suggest that the time fluctuation and average position adopted by the H1–H3 loop affect the ability of GR LBD-21OH-6,19OP complex to homodimerize, a necessary step in transcriptome assembly. A nuclear localization and a transactivation experiment showed that, although 21OH-6,19OP activates the translocation of the GR, the nuclear complex is unable to induce the transcription of a reporter driven by a promoter, that requires binding to a GR homodimer to be activated. These findings support the hypothesis that the passive antagonist mode of action of 21OH-6,19OP resides, at least in part, in the incapacity of the GR–21OH-6,19OP complex to dimerize.

### Introduction

Glucocorticoid receptors (GRs)<sup>a</sup> are members of the steroid–thyroid–retinoid superfamily of nuclear receptors (NR). These are soluble, intracellular receptor proteins that act as ligand-regulated transcription factors controlling specific gene expression in most mammalian cells.<sup>1</sup> In mammals, the NR superfamily includes 48 proteins that are essential in embryonic development, maintenance of differentiated cellular phenotypes, metabolism, and apoptosis. The GR, the mineralocorticoid (MR), the progesterone (PR), the androgen (AR), and the estrogen (ER) receptors form a single family called steroid receptors. Phylogenetic analysis and sequence alignments of these receptors show that the first four belong to a subfamily of oxosteroid receptors which differ from the ER subfamily.<sup>2</sup> There is certain promiscuity among different ligands which may be able to bind to a certain oxosteroid receptor. Thus, although cortisol is the GR endogenous ligand in most mammals, it is also able to bind to the MR with high affinity.<sup>3</sup> In a similar way, progesterone, the PR endogenous ligand, exhibits also a strong antimineralocorticoid activity.<sup>4</sup> This promiscuity, also termed cross-reactivity, must be taken into account in drug design of hormonal steroids.

In the absence of hormone, the GR resides in the cytoplasm as a multiprotein complex composed of chaperone proteins

hsp90 and hsp70, immunophilins, FKBP, CyP-40, P23 and possibly a few others. Chaperone hsp90 maintains the GR in a favorable conformational state required for high-affinity ligand binding and cytoplasmic retention. Binding of ligand to the cytoplasmic GR induces the release of hsp90, resulting in conformational changes that lead to GR translocation to the nucleus, where it modulates gene expression through two main modes of action.<sup>5</sup> A direct mechanism involves GR homodimerization and the subsequent binding to hormone response elements (HRE) located in the promoter region of target genes. As a result, GR dimers lead to transcription activation or repression. On the other hand, the activated GR may function through an indirect mechanism in which the GR monomer interacts with other transcriptional factors, such as NFκB, AP-1 or STAT5, without binding to DNA; in this case, the GR controls gene expression by modulating the transcriptional activities of those factors.<sup>1</sup>

The pleiotropic effects of glucocorticoids (GCs) include their participation in many physiological processes such as endocrine homeostasis, stress responses, lipid metabolism, inflammation, and apoptosis.<sup>1</sup> New insights into the molecular mechanisms of glucocorticoid-mediated actions have provided opportunities for identification of substances with a better therapeutic index. Drugs acting at the glucocorticoid receptor, either as agonists or antagonists, are used in a wide variety of clinical indications. Synthetic glucocorticoids, such as dexamethasone (**1**) (Chart 1) or prednisolone, are widely used in the treatment of several conditions, including asthma, rheumatoid arthritis, and allergic rhinitis. However, the desired antiinflammatory and immunosuppressant effects are often accompanied by severe and/or partially nonreversible side effects (e.g., diabetes mellitus, Cushing's syndrome, osteoporosis, skin atrophy, psychosis, glaucoma, and many others). Moreover, glucocorticoids are also used as adjuvants as they alleviate acute toxic effects in healthy tissue; however they also induce treatment resistance in solid tumors,<sup>6,7</sup> an undesired secondary effect. Currently, it is accepted that the beneficial effects of glucocorticoids may be associated to indirect-transrepression mechanisms while the side effects are

\* To whom correspondence should be addressed. Phone/Fax: 54-11-4576-3385. Email: burton@qo.fcen.uba.ar.

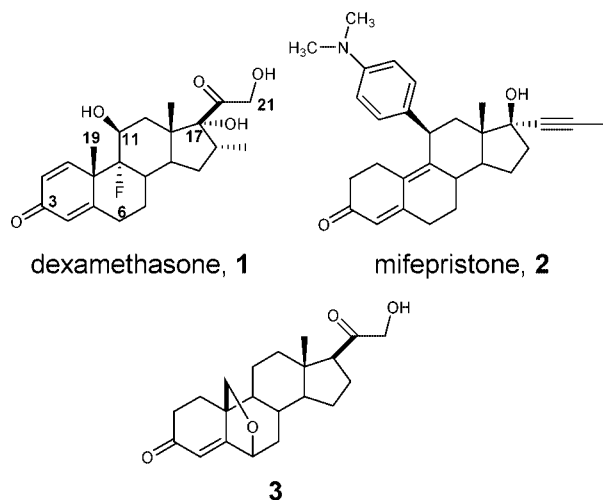
<sup>†</sup> Departamento de Química Orgánica/UMYFOR-CONICET.

<sup>‡</sup> Departamento de Química Inorgánica, Analítica y Química Física/INQUIMAE-CONICET.

<sup>§</sup> Departamento de Química Biológica/IFIBYNE-CONICET.

<sup>a</sup> Abbreviations: GR, glucocorticoid receptor; NR, nuclear receptor; MR, mineralocorticoid receptor; PR, progesterone receptor; AR, androgen receptor; ER, estrogen receptor; HRE, hormone response element; dex, dexamethasone; AF-1, activation function-1 domain; DBD, DNA binding domain; GRE, glucocorticoid response element; LBD, ligand binding domain; LBP, ligand binding pocket; AF-2, activation function-2 domain; 21OH-6,19OP, 21-hydroxy-6,19-epoxyprogesterone; TAT, tyrosine aminotransferase; MD, molecular dynamics; RXR, retinoid X receptor; ED, essential dynamics; DMEM, Dulbecco's Modified Eagle's Medium; CS, calf serum; MMTV, mouse mammary tumor virus; PBS, phosphate-buffered saline; RESP, restraint electrostatic potential.

## Chart 1. Structures of GR Ligands



associated to direct transactivation mechanisms.<sup>8</sup> Intense efforts are being made to identify new glucocorticoids that are able to interact specifically with the GR (selective glucocorticoids), as well as glucocorticoids that are able to differentially modulate GR to retain the transrepression action but without the transactivation action (dissociated glucocorticoids). Antiglucocorticoids (ligands that block the agonist action) also have a large number of clinical applications, the most common indications being for treatments of Cushing's syndrome, GC dependent hypertension, depression and glaucoma. At present, the only available antiglucocorticoid agent is mifepristone, **2** (RU-486) (Chart 1) developed in 1981,<sup>9</sup> but this compound is better known for its antiprogesterin activity.<sup>10</sup>

Like most of the NRs, the GR is a modular protein that is organized into three major domains: a poorly conserved N-terminal activation function-1 domain (AF-1) containing a ligand-independent transcriptional activation function (constitutive transcription enhancement), a highly conserved central DNA-binding domain (DBD) containing two zinc-finger motifs that recognize specific palindromic sequences (glucocorticoid response elements or GREs) in target gene promoters, plus a dimerization region, and a C-terminal ligand-binding domain (LBD).<sup>5,11</sup> The LBD of NR is typically 250 amino acids long containing 12 helices that fold into a globular structure consisting of three sets of helices that form the sides and top of the globule. Three key elements are relevant: the ligand binding pocket (LBP), the dimerization interface and a domain involved in the corepressors and coactivators recognition named AF-2 (Figure 1). In this way, LBD is the most relevant domain to be considered in the design of more specific agents.

The arrangement of helices creates a free residue cavity in the bottom half of the GR LBD where the ligand molecule is bound. This ligand binding pocket of steroid receptors consists of ca. 75% hydrophobic residues, and according to the X-ray structure of GR LBD bound to dexamethasone, all polar residues are involved in hydrogen bonds to the ligand.<sup>12</sup> The volume of the steroid receptor pocket is variable and can change significantly depending on the size and shape of the bound ligand.<sup>2</sup> Receptor dimerization in steroid receptors is mediated in part through the LBD (high homodimerization site), and in part through the DBD (low homodimerization site). In GR LBD the interface involves the formation of a central hydrophobic core between  $\beta$ -sheets and the formation of intramonomer hydrogen

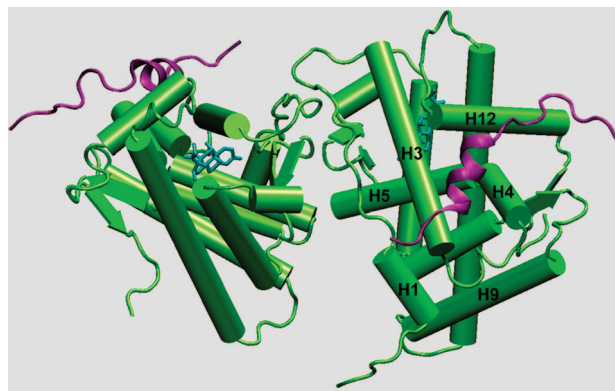


**Figure 1.** General view of the crystal structure of the GR LBD dimer (pdb code: 1M2Z), showing the two LBDs (green), the two coactivator peptides (purple) and the two dexamethasone molecules (cyan).

bonds.<sup>8,12</sup> The ability of agonists to induce an adequate homodimerization is a critical point to achieve transactivation activity.

The AF-2 domain is a hydrophobic site groove conformed by helices H3, H4 and the C-terminal H12. Upon ligand binding, this domain adopts a specific conformation which is able to recruit coactivators. The coactivators bind to LBD via LxxLL sequence motifs (termed NR-boxes) found in multiple copies within the coactivator protein. This short peptide motif is typically helical, and the leucine residues are presented on one face of the amphipathic helix making it to contact with the nonpolar groove of AF-2. Additional electrostatic interactions, termed "charge clamp", between aminoacid side chains of the receptor and the peptide backbone are involved in LBD-coactivators complex orientation and stability. Binding of a coactivator is believed to be one of the key events in initiating transcriptome assembly and subsequent transcription.<sup>2,11</sup>

X-ray crystallographic studies of NR LBD showed that the conformation of the AF-2 domain is mainly determined by the position of H12. In the active conformation, the H12 spans across H3 and H4 creating an adequate surface for docking of coactivators. Several antagonists have a bulky side chain that cannot be contained within the LBP and protrudes out of the LBD preventing H12 from adopting the agonist-bound conformation (active antagonism). Binding of these antagonists, e.g., **2** for GR,<sup>13</sup> can then shift the H12 helix to a different position modifying the docking surface conformation and blocking the coactivator peptide binding-site of the receptor.<sup>14,15</sup> However, there are a number of antagonists dubbed passive antagonists,<sup>16</sup> that do not contain the prototypical side chain found in the active antagonists. Examples of passive antagonists of steroids receptors are, among others, flutamide for AR,<sup>17</sup> 4-hydroxytamoxifen and the *R,R* enantiomer of 5,6,11,12-tetrahydrochrysen-2,8-diol for ER,<sup>15,16</sup> progesterone for MR,<sup>18</sup> and cyproterone acetate for GR.<sup>19</sup> These ligands are similar in size to the corresponding endogenous agonists and do not present a protruding bulky group that may interfere with the positioning of H12. Thus, a different molecular basis has been proposed to explain the antagonistic behavior of this type of ligands, involving the stabilization of nonproductive conformations of key residues.<sup>16,19</sup>

There have been numerous interesting studies demonstrating that ligand binding does not simply trigger NRs from an off-state to an on-state. In fact, these studies revealed at a molecular level that the activation or deactivation of a specific NR upon ligand binding, would be dramatically more complex than a two-state process. In this sense, to understand the molecular mechanisms involved in the complex regulation of NR activity,

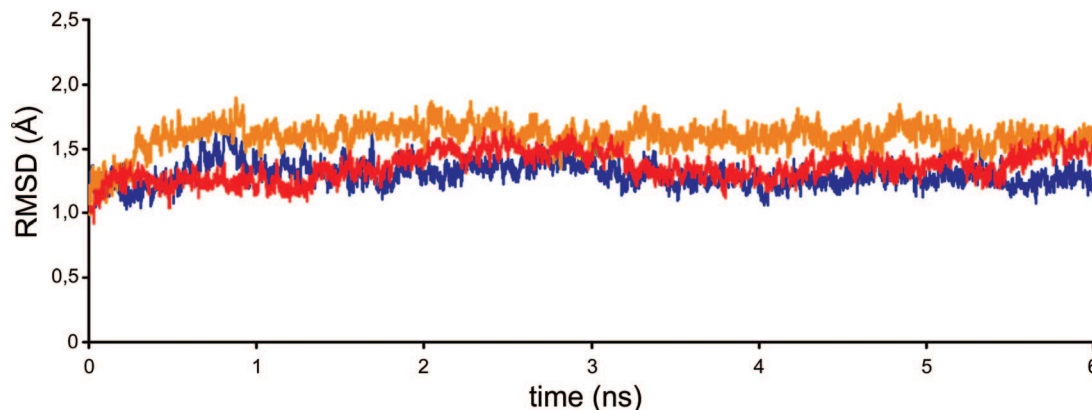


**Figure 2.** Root mean squared deviation (rmsd) from the initial structures measured over the backbone atoms of the simulated system (GR–dex in red; GR–21OH-6,19OP in blue, and GR apo system in brown).

it is necessary to consider that the receptor can also adopt several intermediate conformations upon ligand binding. In this way, the GR–ligand complex activity would depend on the set of proteins (coactivators, corepressors or specific transcription factors) able to interact with a specific GR–ligand complex conformation.

Opposing conformational characteristics for glucocorticoids and mineralocorticoids were described by Weeks et al. who used X-ray diffraction to demonstrate that optimal glucocorticoid properties could be obtained with corticoids exhibiting a torsioned A ring toward the  $\alpha$  face of the steroid nucleus.<sup>20</sup> Previous work from our group has shown that 21-hydroxy-6,19-epoxyprogesterone, **3** (21OH-6,19OP) (Chart 1), is a highly selective antiglucocorticoid devoid of mineralocorticoid and progestational activities.<sup>21</sup> The absence of a bulky side chain in this compound was indicative of passive antagonism. In  $\Delta^4$ -steroids such as 21OH-6,19OP, the 6,19-epoxy bridge bends the steroid skeleton at the A/B ring junction stabilizing the quasi-cis conformation with an inverted ring A  $1\beta$  half-chair, a structural characteristic also present in the antiglucocorticoid and antiprogestagen mifepristone (**2**).<sup>22</sup> The crystal structure of the glucocorticoid receptor–ligand binding domain in complex with **2**, shows the latter molecule with its ring A exaggeratedly bent toward the  $\alpha$  face, in a distorted conformation that closely matches that of 21OH-6,19OP.<sup>23</sup> However, at variance with **2**, which is a flexible molecule, 21OH-6,19OP (**3**) has a rigid structure that locks the conformation of ring A. The 21OH-6,19OP efficiently displaces [<sup>3</sup>H]corticosterone from thymus-glucocorticoid receptors but competes with neither [<sup>3</sup>H]aldosterone for kidney-mineralocorticoid receptors nor [<sup>3</sup>H]progesterone for uterus-progesterone receptors.<sup>21</sup> It is unable to induce tyrosine aminotransferase (TAT) or to increase glycogen deposits in rat liver but, when coincubated with corticosterone or dexamethasone, 21OH-6,19OP (2.5  $\mu$ M) inhibits 80% of TAT induction. It has also been used to explore the mechanism of cortisol/progesterone antagonism in the regulation of 15-hydroxyprostaglandin dehydrogenase activity.<sup>24</sup>

Central to the understanding of the molecular role played by different ligands on coactivator recruitment and dimer formation is the ability of predicting the overall conformation change and the overall stability of the receptor upon ligand binding. Crystallographic studies of NRs have provided essential but not conclusive information about the molecular basis of action, since crystal structures represent only extreme states of the configurational space of the receptor–ligand complex and the dynamic behavior cannot be determined. Molecular dynamics (MD) simulations are one of the most versatile and widely applied

computational techniques for the study of biological macromolecules. They are very valuable for understanding the dynamic behavior of proteins at different timescales, from fast internal motions to slow conformational changes or even protein folding processes.

### Molecular Dynamics Simulations of GR–Ligand Complexes

To investigate the molecular basis of the passive antagonism exhibited by 21OH-6,19OP, we performed MD simulations on three different binding states of GR LBD: an agonist system (dex), an antagonist system (21OH-6,19OP), and an unbound system (apo). It is well-known that, at the molecular level, the interaction between two proteins is determined either by the overall structure of each of them and/or by their dynamical behavior. We evaluated and compared these two properties in the three different conformational states of GR LBD (dex system; 21OH-6,19OP system and apo system) and determined the average structures and the residue fluctuation from MD simulation.

**Stability of MD Simulation.** We started our analysis by inspecting the stability along the 6 ns MD runs. Visual inspection of all structures shows that the global folding remains essentially intact, and the time-dependent residue fluctuation (root-mean-square deviations, rmsd) measured over the backbone atoms from the initial structures reveals that simulations are reasonably stable (Figure 2). The average rmsd were  $1.35 \pm 0.11$ ,  $1.30 \pm 0.9$ , and  $1.68 \pm 0.12$  Å for dex, 21OH-6,19OP, and apo systems respectively, suggesting that the apo structure undergoes more conformational changes than holo receptors. Thus, fast changes in the receptor structure are caused by the lack of ligand in LBP during the first nanosecond and then remains essentially stable until 6 ns.

**Ligand Binding Mode. (i) Dex System.** The ligand-binding site of GR is lined by residues 560, 563, 564, 567, and 570 from H3, 600, 601, 604, 605, 608, and 611 from H4–H5, 642, and 646 from H7, 732, 735, 736, and 739 from H11, 747, and 749 from H11–H12 loop and residue 753 from H12. Five of these residues (Gln570, Arg611, Asn564, Thr739, and Gln642) are polar residues able in principle, to form hydrogen bonds with the ligand. The remaining amino acids may experience hydrophobic interactions with the carbon skeleton of the steroid. Figure 3a displays the hydrogen-bond contacts between ligand and receptor and the percentage of time in which hydrogen bonds are formed during the time scale of the MD simulation of the dex system. Two very stable interactions were observed



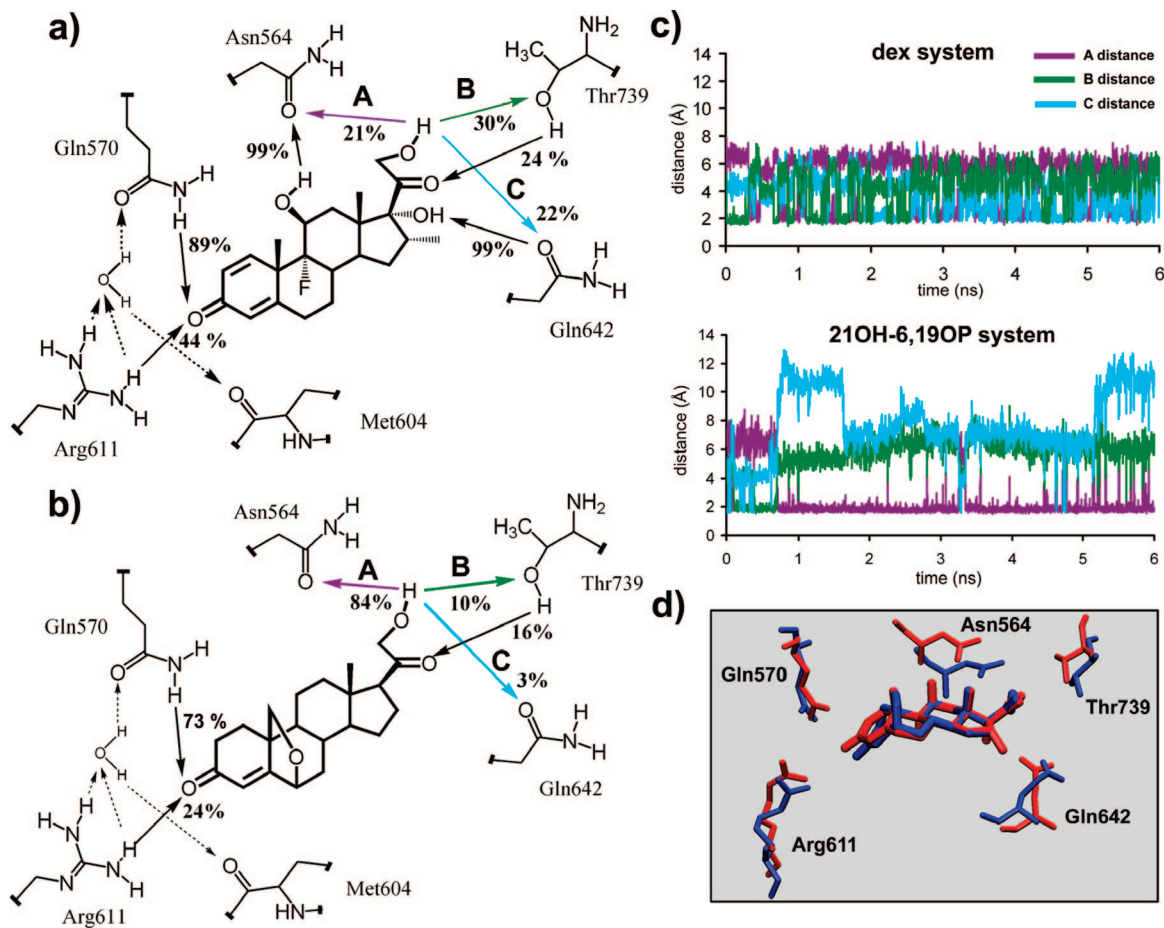


**Figure 3.** Comparison of ligand binding mode of (a) dex (1) and (b) 21OH-6,19OP (3) showing a schematic representation of the polar interactions of ligands with the LBP of GR LBD. Hydrogen bond contacts are shown as arrows, and numbers near the arrows correspond to the percentage of time in which hydrogen bonds are formed during the time scale of our MD simulations. (c) Time evolution of the distance between ligand 21-hydroxylic proton and eventual H-bond acceptor atoms of Asn564, Thr739, and Gln642. Distances smaller than 2.5 Å indicate that strong and stable H-bonds are formed. (d) Detailed view of the carbon skeleton of ligands next to polar residues of LBP, performed by superimposing ring C of the average structure of the steroids over the last 4 ns of the MD simulation (GR-dex in red; GR-21OH-6,19OP in blue).

during almost all the MD simulation: the 17 $\alpha$ -hydroxyl with Gln642 and the 11 $\beta$ -hydroxyl with Asn564. These strong and stable interactions, also observed in the crystal structure,<sup>12</sup> play a fundamental role in ligand-receptor recognition and since both hydroxyl groups are present in the natural glucocorticoid (cortisol) a conserved role must be considered. The C-3 carbonyl group participates on a hydrogen bonding network that involves the Gln570, Arg611 and a water molecule. The water molecule does not directly form a hydrogen bond with the steroid, but stabilizes the Gln570 and Arg611 conformation in an appropriate position, that allows interaction with the oxygen atom of the ligand. Exchange of water molecules has been observed throughout the MD simulation, however the position and binding mode with Gln570 and Arg611 remains virtually unchanged. This water molecule is not present in the X-ray structure; however other simulations of steroid LBDs have shown the same behavior.<sup>25,26</sup> In this hydrogen-bonding network, the ligand forms a very stable hydrogen bond with Gln570 and a less frequent one with Arg611.

In solution, the conformation of the 17 $\beta$  side chain of dexamethasone is not restricted, with the 21-hydroxy group moving freely. In contrast, the MD simulation shows that, within GR LBD, the orientation of the 21-hydroxyl alternates between three well defined positions determined by three different hydrogen bond interactions between the 21-hydroxyl and residues Asn564, Thr739 and Gln642 (Figure 3c). Each of these

hydrogen bonds has similar frequency, indicating that in this system this group has no preferential orientation.

**(ii) 21OH-6,19OP System.** The molecule was introduced in the LBP superimposing the carbon atoms of the C ring with the equivalent atoms of the dex ligand. Visual inspection of the overall position shows that this molecule practically stays in its original position during simulation. The 21OH-6,19OP molecule has only three groups capable of forming hydrogen bonds with the receptor: the oxygen atom of the 6,19-epoxy bridge, and the carbonyl oxygens at C-3 and in the 17 $\beta$  side chain. As mentioned above, the latter two groups are also present in the dex ligand, but interestingly, important differences were observed in the mode of interaction of the receptor with 21OH-6,19OP.

A similar hydrogen-bonding network around the C-3 carbonyl group was observed in both systems (dex system and 21OH-6,19OP system) (Figure 3a,b). As in the case of the dex system, an exchangeable water molecule interacts with residues Arg611, Gln570 and Met604 forming hydrogen bonds with Gln570 and Arg611. However, as 21OH-6,19OP has a more tensioned structure, the oxygen atom at C-3 is further away from the nitrogen atom of Arg611, forming less frequently a hydrogen bond compared with the dex system. Moreover, this ligand conformation allows after 4 ns, the incorporation of a second water molecule between the Gln570 and the C-3 carbonyl of the ligand, which interacts through a hydrogen bond with both

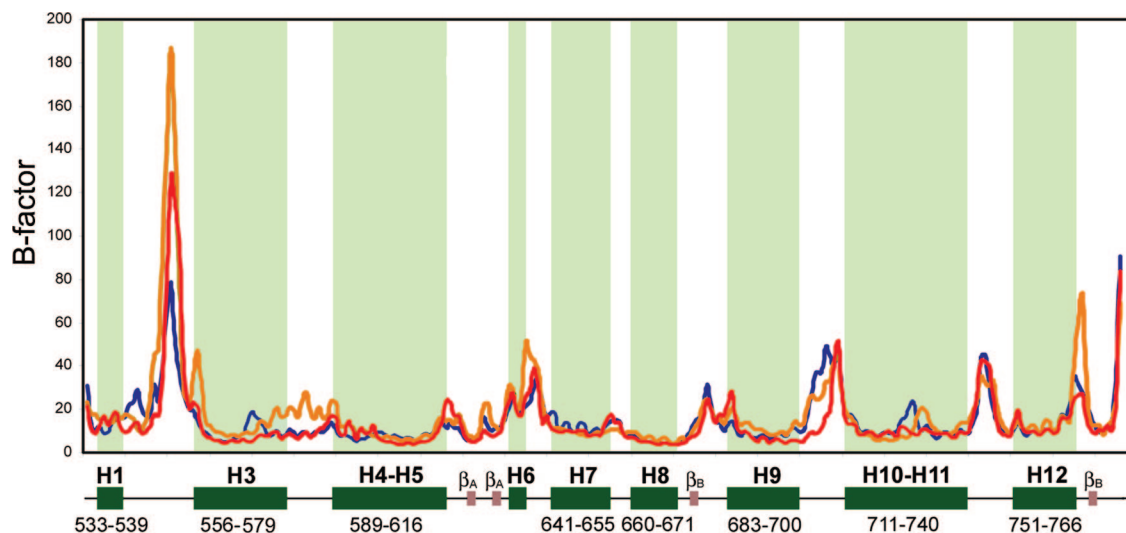


**Figure 4.** Comparison of B factors of the three systems over the last 4 ns of MD simulation (GR–dex in red; GR–21OH-6,19OP in blue, and GR apo system in brown). The secondary structure of GR LBD is schematized along the *x*-axis.

the protein and the ligand (data not shown). Despite this fact that causes a decrease in the frequency of the C-3 carbonyl-Gln570 direct interaction, no major structural changes were observed in the LBP or in the rest of the receptor molecule.

In contrast to the dex system, the 21-hydroxyl of 21OH-6,19OP does not alternate between three well defined positions. After the first stage of the simulation, this hydroxyl interacts through a hydrogen bond with Asn564. This hydrogen bond interaction remains stable during the rest of the simulation (Figure 3c). Thus, this preferential orientation of the 21-hydroxyl in the 21OH-6,19OP system is reflected in the higher frequency of hydrogen bonding with Asn564. Two key features are decisive in determining the different hydrogen bonding pattern of the 21-hydroxyl in the 21OH-6,19OP and dex systems. First, the intramolecular bridge in 21OH-6,19OP bends the steroid skeleton giving a shorter molecule. This is consistent with the fact that HF/6-31G\*\* geometry optimizations predict that the C3–C17 distance is 8.23 Å for dex and 7.71 Å for 21OH-6,19OP. As a result, the 21-hydroxyl is further away from the Thr739 and Gln642 residues but nearer to Asn564. Second, the lack of an 11-hydroxyl allows Asn564 to acquire a more favorable orientation to interact with the 21-hydroxy group.

Examination of the LBP around the 6,19-epoxy bridge of 21OH-6,19OP shows that there are no polar residues capable of forming hydrogen bonds with the oxygen atom; thus, no appreciable changes associated to this bridge occurred during the simulation. In summary, by analyzing at a molecular level the ligand binding mode of the holo systems, we have found that important differences exist, especially in the disposition of the polar residues of LBP (Figure 3d).

**Overall Backbone Fluctuations.** To study the dynamical behavior of the protein after reaching an equilibrium state, we calculated the B-factors of the three simulated systems, which provide a time-average representation of per-residue fluctuations, over the last 4 ns of MD simulation. Figure 4 show that all systems displayed a similar fluctuation pattern. As expected, regions with larger B-factors correspond to loop regions in all structures while the helices, that are more structured regions, present smaller B-factor values. However, detailed comparison of B-factors between systems reveals significant differences, mainly in two regions. First, despite the fact that residues around 551 fluctuate much more than the rest of the protein, this fluctuation is more pronounced in the apo and dex systems

compared to the 21OH-6,19OP system. Structural and dynamic analysis of this region of GR LBD is very important since it corresponds to terminal regions of the H1-H3 loop, that participate actively in homodimerization of GR LBD. Second, the B-factor of the C terminal region of H12, which is involved in the AF-2 conformation, is larger in the apo receptor than in the holo receptors.

**Dimer Interface.** As found for the progesterone receptor,<sup>27</sup> the available crystal structures of GR LBD also reveal a distinct dimerization interface that differs from that present in ER and retinoid X receptor (RXR).<sup>12,23</sup> While in the latter receptors dimerization occurs predominantly through H10 with contributions from H7, H8 and H9,<sup>14,28</sup> the GR LBD dimer interface involves residues Pro625 and Ile628 of the  $\beta$ -sheet located between H5 and H6 and the residues 547 to 551 of the H1-H3 loop (Figure 1). Pro625 and Ile628 of one monomer contact the same residues of the other, forming a core hydrophobic interface. Around this core, residues 547 to 551 from each LBD adopt an adequate geometry facilitating the inter monomer interaction through four hydrogen bonds.<sup>8,12</sup> The functional significance of this dimer interface is supported by mutagenesis studies, thus mutation of residue Ile628 resulted in decreased GR-mediated transactivation but did not affect transrepression.<sup>12</sup> When comparing the average structures of the GR LBD-dex and GR LBD-21OH-6,19OP complexes, two main differences were observed: the conformation adopted for the H1-H3 loop and the conformation of H12. No significant changes were observed in other regions of the complexes. Our simulations suggest that, depending on the LBP state, important structural changes of the H1-H3 loop occurred during the MD simulation. Inspection of the time average structures reveals clearly the distinct conformation adopted for this loop in each system (Figure 5), this figure shows that the average position of this loop in the apo system is modified significantly with respect to the protein complexed with ligands. The presence of dex leads to a GR LBD conformation in which the N-terminal region of H1-H3 loop is close to the protein body; on the other hand, when 21OH-6,19OP is present, this loop is located further away from the rest of the protein.

To further characterize the dynamical behavior of GR LBD, we performed an essential dynamics analysis (ED) for the three systems over the last 4 ns of MD. The ED analysis showed that in either the apo or dex system there is an essential mode

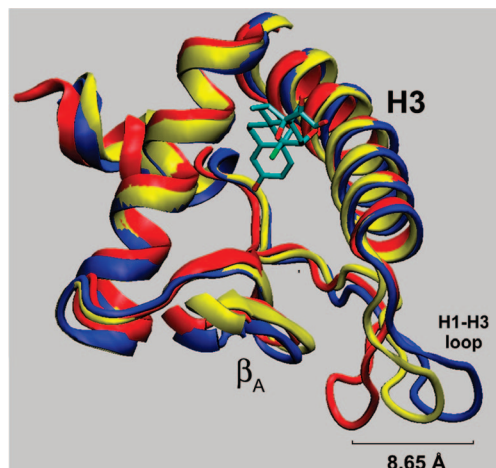


**Figure 5.** H1-H3 loop average structure of the three systems (GR-dex in red; GR-21OH-6,19OP in blue, and GR apo system in yellow) taken over the last 4 ns of MD simulation. The ligand shown is dexamethasone in GR-dex.

that accounts for nearly 50% of the total protein motion. The movement along this mode is localized in the H1-H3 loop. Interestingly, this loop is the one which exhibits the more significant structural differences among the considered systems, as shown in Figure 5. In the 21OH-6,19OP system the first mode also involves the dimerization loop, but it only accounts for 20% of the total motions, indicating a minor mobility of these residues with respect to the apo and the dex system. In summary, we have observed that the average position of the H1-H3 loop and its dynamical behavior depend strongly on the LBP state. In the agonist state (dex system), the H1-H3 loop fluctuates moderately around a position close to H6; in the apo state (without ligand), the fluctuations of the H1-H3 loop are greater and the average position is further positioned toward H6. Finally, in the antagonist state (21OH-6,19OP system), the loop immediately evolves to a rigid conformation even further away from the body of the protein.

**AF-2 Domain.** Either X-ray structures or MD simulation studies on the NR LBD have shown that mutations, binding of antagonist or simply the lack of ligand can cause large conformational changes in the H12 helix. These conformational changes consist, for example, in significant reorientations (around  $130^\circ$ ) with respect to the “active” conformation<sup>14</sup> or even the complete loss of the helix motif.<sup>23</sup> As GR LBD has many features in common with other NRs, it would be expected a similar H12 dynamic behavior. However, GR LBD has an additional  $\beta$ -sheet (conformed by residues 769–771 of the GR LBD N-terminal region and residues 674–676 located between H8 and H9), which plays an important role in stabilizing the H12 in the AF-2 conformation. Interestingly, despite the fact that in the GR LBD-mifepristone crystal structure the H12 is not solved, this additional  $\beta$ -sheet is present.<sup>23</sup> Thus, as the mobility of the H12 is limited, a different behavior should be expected upon ligand binding.

Remarkably, our MD simulations show that there is a connection between the conformation-fluctuation pattern of the GR LBD N-terminal residues and the receptor state. The last 4 ns average structures clearly reveal that in the 21OH-6,19OP system, the residues 762–767, originally located in a loop region, adopt a more structured conformation (Figure 6a). In other words, residues 762–767 acquire a helix motif, making H12 longer by five residues compared to the original structure. In contrast, in the dex system, the conformation of these residues

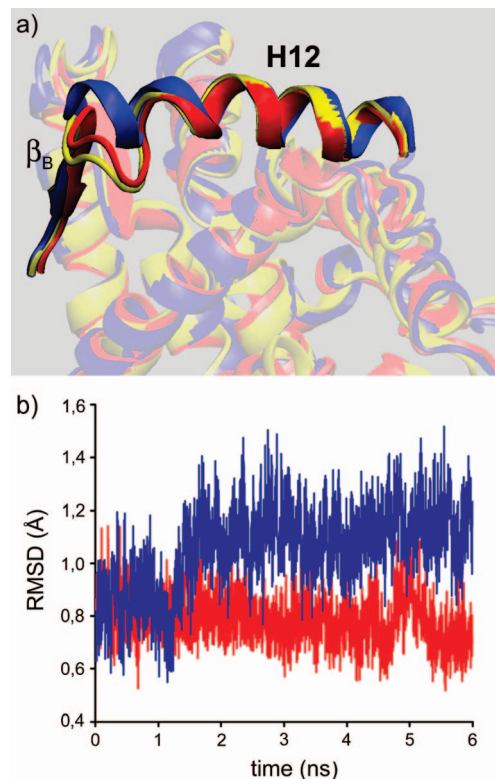


**Figure 6.** (a) H12 average structure of the three systems (GR-dex in red; GR-21OH-6,19OP in blue, and GR apo system in yellow) taken over the last 4 ns of MD simulation. (b) Root mean square deviation (rmsd) of H12 (residue 750–768) from the initial structures measured over the backbone atoms of the GR-dex (red) and GR-21OH-6,19OP (blue) systems.

remains very close to that observed in the original state. rmsd of H12 measured over the backbone atoms from the initial structure indicates that this change is not a gradual process, but a rmsd jump occurs around 1.4 ns (Figure 6b). After that, this rigid helix conformation remains stable, explaining the low B factor observed (Figure 4). Despite the fact that the average position and conformation of residues 762–767 in the apo system is similar to the one observed in the dex system, an increase in the fluctuation of 762–767 residues occurs (Figure 4). Since the H12 and the  $\beta$ -sheet structures are essential elements on the regulation of the AF-2 conformation, we see again, that a fundamental region of the GR LBD activity is strongly dependent on the LBP state.

In addition to the hydrophobic interaction between leucines of LxxLL motif of coactivators and the groove of AF-2 domain, there are two electrostatic interactions termed “charge clamp”. One of this is also observed in other NRs and is conformed by the residues Lys579 and Glu755. The second one is a distinctive feature of the GR LBD and is conformed by the second pair of polar residues, Arg585 and Asp590.<sup>12</sup> Both charge clamps are involved in the electrostatic interaction between the receptor and specific coactivators such as SRC-2 (Figure 7).

In this way, the relative position between these four residues determines the accessibility opening dimension of the AF-2 groove. To investigate the influence of the ligand on this GR LBD region, we measured the average C $\alpha$  distances among these four residues for the dex and the 21OH-6,19OP systems (Table 1). Interestingly, we found that the C $\alpha$  distances that differ appreciably (dex system ca. 0.6 Å larger than the 21OH-6,19OP system) are those in which the only residue located in H12 (Glu755) is involved, while the C $\alpha$  distances among the



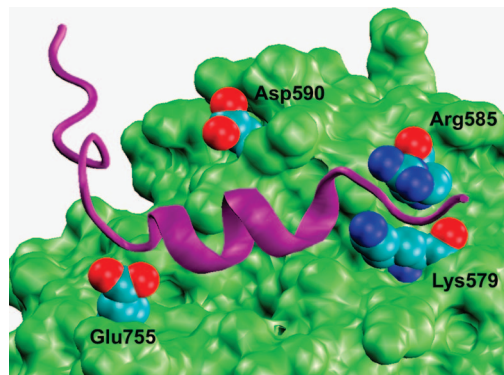


**Figure 7.** Detailed view, taken from the crystal structure of GR LBD dimer (pdb code: 1M2Z), of the AF-2 domain of GR LBD (green) and residues (oxygen atoms in red, carbon atoms in cyan and nitrogen atoms in blue) that form the charge clamps involved in the electrostatic interaction between the receptor and the SRC-2 coactivator (purple).

**Table 1.** C $\alpha$ -C $\alpha$  Distances among the Four Residues That Form the Charge Clamps in GR-dex and GR-21OH-6,19OP Complexes

residue		C $\alpha$ -C $\alpha$ distance (Å)		
<i>i</i>	<i>j</i>	GR-dex	GR-21OH-6,19OP	$\Delta$
755 (H12)	579 (H3)	19.38	18.90	0.48
755 (H12)	585 (H3-H4 loop)	22.59	21.99	0.60
755 (H12)	590 (H4)	15.79	15.18	0.61
579 (H3)	585 (H3-H4 loop)	5.30	5.29	0.01
579 (H3)	590 (H4)	10.80	10.83	-0.03
590 (H4)	585 (H3-H4 loop)	10.92	10.91	0.01

other residues do not depend significantly on the ligand structure bound to the GR LBD. These results show that the ligand structure would affect not only the stability of the H12 backbone in the AF-2 conformation, but also the accessibility of the AF-2 groove, suggesting a fine regulation in the ability of the receptor to recruit a specific coactivator.

### Nuclear Localization and Transactivation Activity of the GR-21OH-6,19OP Complex

According to the above calculations, 21OH-6,19OP should form a stable complex with GR that cannot dimerize. However, nothing can be said on the ability of this complex to translocate to the nucleus and eventually participate in those mechanisms that involve monomeric activated GR. Thus we carried out a set of experiments aimed to show if 21OH-6,19OP is able to induce GR transformation and translocation from cytoplasm to the nucleus and also, to give us some insight on the capacity of that receptor complex to dimerize.

We used L929 cells derived from mouse fibroblast which express endogenous GR to perform confocal microscopy of immunofluorescence analysis. Figures 8 panels a-d show that the GR is localized in both, the cytoplasm and the nucleus of untreated L929 cells (panel a). When cells were incubated with dex, GR was mainly in the nucleus (panel b). GR also localized in the nucleus in both, L929 cells treated with dex plus 21OH-6,19OP (panel c) or with 21OH-6,19OP alone (panel d), showing that this synthetic ligand is able to induce transformation-translocation of the receptor. Taken together, these experimental results support the assumption that 21OH-6,19OP impairs GR activation after its translocation and are consistent with the calculation results.

To evaluate the dimerization ability of the GR-21OH-6,19OP complex, we analyzed its transactivation activity by transfecting the reporter pMMTV-luciferase vector in L929 cells.<sup>29</sup> The

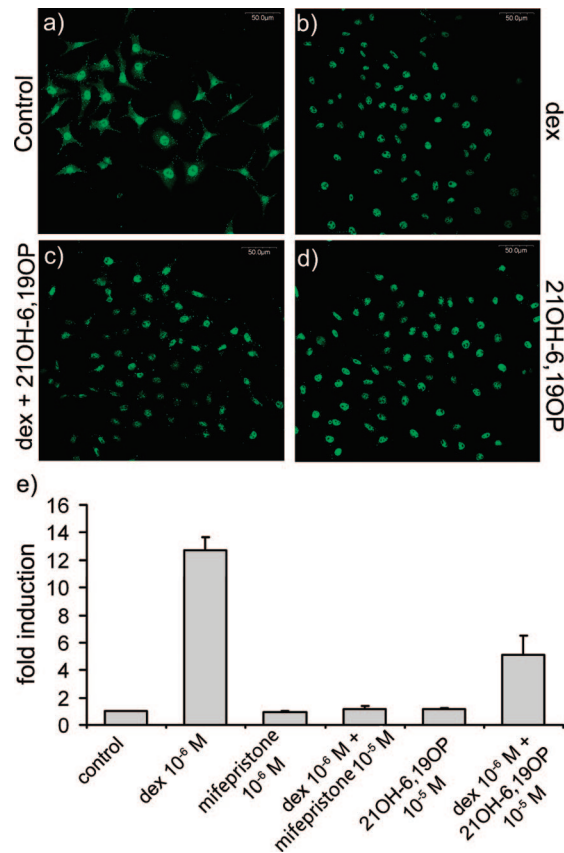


**Figure 8.** Fluorescence confocal microscopy. L929 cells were incubated for 30 min with (a) ethanol (control), (b) dex 1  $\mu$ M, (c) dex 1  $\mu$ M + 21OH-6,19OP 10  $\mu$ M, and (d) 21OH-6,19OP 10  $\mu$ M. They were then immunolabeled for GR and analyzed by laser fluorescence confocal microscopy. Magnification,  $\times 400$ . Bar, 50  $\mu$ m. Results are representative of three independent experiments. (e) L929 cells were transfected with 3  $\mu$ g of MMTV-Luc reporter vector. One microgram of pCMV-LacZ vector was also introduced. Cells were incubated for 24 h as indicated, and luciferase activity was measured. After correcting for  $\beta$ -galactosidase activity, the values are expressed as fold induction relative to the control. The means  $\pm$  SE from three independent experiments are shown.

MMTV promoter contains glucocorticoid specific response elements able to bind GR activated homodimers.<sup>30</sup> Luciferase activity was measured in this cell line as a downstream expression of the responsive receptor activities, in the presence of 10<sup>-5</sup> M 21OH-6,19OP alone or together with 10<sup>-6</sup> M dexamethasone. The results presented in Figure 8e show a significant inhibiting effect of 21OH-6,19OP on the glucocorticoid action of dexamethasone ((5.1  $\pm$  1.4)- vs (12.7  $\pm$  0.9)-fold induction with respect to the control, comparing lane 6 vs lane 2), however this inhibition is lower than that observed in cells treated with dexamethasone plus **2** ((1.2  $\pm$  0.2)-fold induction, compare lane 6 with lane 4). On the other hand, 21OH-6,19OP alone had no glucocorticoid effect per se (1.2  $\pm$  0.1, lane 5). These effects are in agreement with those previously mentioned for the induction of TAT. Thus, these results suggest that 21OH-6,19OP may affect the ability of GR to induce transcription at least as an homodimer, impairing the direct transactivation of target genes.

### Conclusions

A current goal in hormonal steroid drug discovery is to manipulate the steroid receptor activity by designing ligands that are able to retain tissue-selective benefits while minimizing

unwanted activities. To understand how a specific ligand modulates the conformation and dynamic behavior of its receptor it is necessary to analyze the ligand–receptor interaction at the molecular level. Since there are yet no reports of a crystal structure of a ligand-free steroid receptor, the precise nature of the pocket in the absence of ligand is unknown. However, we believe that the crystal structure of the GR–dex complex is an adequate starting point to evaluate with MD, the properties of other nuclear GR complexes. The medium-range MD simulation of GR LBD–21OH-6,19OP and GR LBD–dex complexes and ligand free GR LBD described above, gives us an insight into the molecular basis involved in the action of the bridged rigid steroid with antiglucocorticoid properties, 21OH-6,19OP. Our results clearly showed that the state of the LBP of GR LBD determines the receptor behavior during the simulation with important differences between the interaction hydrogen bond patterns of GR–21OH-6,19OP and GR–dex. These differences would explain the different behavior of two fundamental regions of GR LBD: the H1–H3 loop and the H12. Remarkably, our MD results suggest that in the GR LBD–21OH-6,19OP complex the average position of the H1–H3 loop would prevent GR homodimerization. The nuclear localization experiment showed that 21OH-6,19OP does not impede GR translocation, but changes the conformation of the nuclear complex making it unable to activate gene transcription. In this sense, our experimental results also show that the GR–21OH-6,19OP complex is unable to induce transcription of MMTV promoter, known to be activated by the recruitment of GR homodimers to specific response elements. These findings taken together, support the hypothesis that the passive antagonist mode of action of the antiglucocorticoid 21OH-6,19OP resides, at least in part, in the incapacity of GR–21OH-6,19OP complex to dimerize. Although how this and other conformational changes affect the interaction of the GR complex with transcription factors still remains unknown, the predicted passive antagonist binding mode may be used as a starting point for the design of new selective antagonists and modulators of the GR and to further unravel the complex underlying mechanisms.

## Experimental Section

**A. Experimental Methods. a. Steroids.** 21-Hydroxy-6,19-epoxyprogesterone (**3**) was prepared as described previously.<sup>31</sup> Dexamethasone (**1**) and mifepristone (**2**) were from Sigma Co. (St. Louis, MO).

**b. Cell Culture and Treatments.** L929 cells were cultured at 37 °C in a humidified atmosphere with 5% CO<sub>2</sub> in DMEM supplemented with 10% calf serum (CS) containing penicillin (100 IU/mL), streptomycin (100 µg/mL) and glutamine (2 mM) in p100 plates. For transient transfections, 5 × 10<sup>5</sup> cells were plated in 60 mm plates and transfected by the lipofectin method according to the manufacturer protocol (Lipofectine Plus, Gibco, Inc.). Analyses of the GR activity were performed by transfecting 3 µg of pMMTV-luc plasmid which expresses luciferase enzyme under the control of Mouse Mammary Tumor Virus promoter containing several HRE elements;<sup>29</sup> 3 µg of pRSV-LacZ (Clontech Inc., Palo Alto, CA) was also introduced as control of transfection. Eighteen hours after transfection, the medium was replaced by new one containing 10% charcoal-stripped CS and antibiotics. Cells were then incubated during 24 h with 10<sup>−6</sup> M dexamethasone with or without 10<sup>−5</sup> M 21OH-6,19OP; 10<sup>−5</sup> M mifepristone was also added as control. Steroids were applied from 1000-fold stock solutions in dimethylsulfoxide. Incubations were stopped by aspirating the medium and washing the cells twice with phosphate buffered saline (PBS). Cells were then harvested in lysis buffer and luciferase activity was measured according to the manufacturer protocol (Promega Inc.). β-Galactosidase activity was measured as previously described.<sup>32</sup>

**c. Confocal Microscopy.** For indirect immunofluorescence studies, L929 cells were incubated for 45 min at 37 °C with 10<sup>−6</sup> M dex with or without 10<sup>−5</sup> M 21OH-6,19OP, and the cells were fixed with 4% paraformaldehyde in PBS for 30 min at room temperature. Cells were permeabilized with 0.1% SDS in PBS for 5 min and washed three times with PBS. Cells were blocked in PBS containing 3% BSA (PBS–BSA) for 30 min at room temperature and then incubated for 2 h at room temperature with an anti-GR antibody (BuGR2 clone, Affinity Bioreagents, Golden, CO) at 1:50 dilution in PBS–BSA. Cells were washed with PBS–BSA and incubated for 30 min with Cy2-conjugated secondary antibody antimouse IgG (492 nm excitation wavelength and 510 nm emission wavelength, catalog no. 711–225–152, Jackson Immuno Research, West Grove, PA, USA) diluted 1:200 in PBS–BSA. Cells were washed three times with PBS and once with distilled water for 5 min. Finally, cells were mounted on a glass slide by adding a drop of 50% glycerol in PBS. Fluorescence was detected with a Weiss LSM 510 laser scanning confocal microscope (Olympus FV300) and images were analyzed with LSM 510 Image Browser software.

**B. Computational Methods. a. Quantum Mechanics Calculations.** The geometries of 21-hydroxy-6,19-epoxyprogesterone and dexamethasone were optimized using the *ab initio* quantum chemistry program Gaussian 03<sup>33</sup> and the HF/6-31G\*\* basis set. RESP (restraint electrostatic potential) atomic charges were calculated for both ligands.

**b. Molecular Dynamics.** Molecular dynamics (MD) were performed by using the AMBER 9 software package.<sup>34</sup> The starting structure for the simulation was taken from the crystal structure of the GR–dexamethasone complex (pdb code: 1M2Z).<sup>12</sup> Since this crystal structure is formed by a homodimer of GR LBD and our purpose was to study the monomer behavior, only chain A was used. The ligand parameters were assigned with the general AMBER force field (GAFF) and the corresponding RESP charges using the Antechamber module of AMBER. The 21OH-6,19OP system was built *in silico*, superimposing carbon atoms of ring C of 21OH-6,19OP with the corresponding atoms of the dex molecule in the GR–dexamethasone complex. To build the apo system, the dex molecule was simply deleted from the GR–dexamethasone complex crystal structure. The complexes were immersed in an octahedral box of TIP3P water molecules using the Leap module, giving final systems of around 27000 atoms. The systems were initially optimized and then gradually heated to 300 K. Starting from these equilibrated structures, MD production runs of 6 ns were performed. All simulations were performed at 1 atm and 300 K, maintained with the Berendsen barostat and thermostat,<sup>35</sup> using periodic boundary conditions and the particle mesh Ewald method (grid spacing of 1 Å) for treating long-range electrostatic interactions, with a uniform neutralizing plasma. The SHAKE algorithm was used to keep bonds involving H atoms at their equilibrium length, allowing us to employ a 2 fs time step for the integration of Newton's equations. The Amber99 force field parameters were used for all residues,<sup>36</sup> except for the above-mentioned ligands. The essential dynamics (ED)<sup>37</sup> for each simulation were determined by diagonalizing the covariance matrices of the atomic positions along the desired trajectory. This allowed us to obtain the eigenvectors corresponding to the essential motions that describe the motion of the protein along the MD run. The ED were computed only for the backbone (N, C, CA) atoms. Terminal residues (523–529 and 773–777) were excluded, since this region was found to be quite flexible, and did not appear to contribute to the structure of the GR LBD fold. Hydrogen bond populations shown in Figure 3 were calculated as the percentage of snapshots where the H-bond was present. A H-bond was defined as present whenever the distance between both heavy atoms involved in the interaction was less than 3.5 Å.

**Acknowledgment.** Financial support by Agencia Nacional de Promoción Científica y Tecnológica, CONICET (Argentina) and Universidad de Buenos Aires is gratefully acknowledged.



**Supporting Information Available:** HF/6-31G\*\*-optimized structures of ligands. This material is available free of charge via the Internet at <http://pubs.acs.org>.

## References

- (1) Necela, B. M.; Cidlowski, J. A. Mechanisms of glucocorticoid receptor action in noninflammatory and inflammatory cells. *Proc. Am. Thorac. Soc.* **2004**, *1*, 239–246.
- (2) Moore, J. T.; Collins, J. L.; Pearce, K. H. The nuclear receptor superfamily and drug discovery. *ChemMedChem* **2006**, *1*, 504–523.
- (3) Farman, N.; Bocchi, B. Mineralocorticoid selectivity: molecular and cellular aspects. *Kidney Int.* **2000**, *57*, 1364–1369.
- (4) Wambach, G.; Higgins, J. R. Antimineralocorticoid action of progesterone in the rat: correlation of the effect on electrolyte excretion and interaction with renal mineralocorticoid receptor. *Endocrinology* **1978**, *102*, 1686–1693.
- (5) Kumar, R.; Thompson, E. B. Gene regulation by the glucocorticoid receptor: structure: function relationship. *J. Steroid Biochem. Mol. Biol.* **2005**, *94*, 383–394.
- (6) Herr, I.; Pfitzenmaier, J. Glucocorticoid use in prostate cancer and other solid tumours: implications for effectiveness of cytotoxic treatment and metastases. *Lancet Oncol.* **2006**, *7*, 425–430.
- (7) Zhang, C.; Beckermann, B.; Kallifatidis, G.; Liu, Z.; Rittgen, W.; Edler, L.; Buchler, P.; Debatin, K. M.; Buchler, M. W.; Friess, H.; Herr, I. Corticosteroids induce chemotherapy resistance in the majority of tumour cells from bone, brain, breast, cervix, melanoma and neuroblastoma. *Int. J. Oncol.* **2006**, *29*, 1295–1301.
- (8) Necela, B. M.; Cidlowski, J. A. Crystallization of the human glucocorticoid receptor ligand binding domain: a step towards selective glucocorticoids. *Trends Pharmacol. Sci.* **2003**, *24*, 58–61.
- (9) (a) Teutsch, J. G.; Costerousse, G.; Philibert, D.; Deraedt, R. *Novel Steroids*. U.S. Patent 4,386,085, 1983. (b) Spitz, I. M.; Bardin, C. W. Mifepristone (RU-486): a modulator of progesterin and glucocorticoid action. *N. Engl. J. Med.* **1993**, *329*, 404–412.
- (10) Zhang, J.; Tsai, F. T.; Geller, D. S. Differential interaction of RU486 with the progesterone and glucocorticoid receptors. *J. Mol. Endocrinol.* **2006**, *37*, 163–173.
- (11) Gronemeyer, H.; Gustafsson, J. A.; Laudet, V. Principles for modulation of the nuclear receptor superfamily. *Nat. Rev. Drug Discov.* **2004**, *3*, 950–964.
- (12) Bledsoe, R. K.; Montana, V. G.; Stanley, T. B.; Delves, C. J.; Apolito, C. J.; McKee, D. D.; Consler, T. G.; Parks, D. J.; Stewart, E. L.; Willson, T. M.; Lambert, M. H.; Moore, J. T.; Pearce, K. H.; Xu, H. E. Crystal structure of the glucocorticoid receptor ligand binding domain reveals a novel mode of receptor dimerization and coactivator recognition. *Cell* **2002**, *110*, 93–105.
- (13) Chen, J. D.; Evans, R. M. A transcriptional co-repressor that interacts with nuclear hormone receptors. *Nature* **1995**, *377*, 454–457.
- (14) Brzozowski, A. M.; Pike, A. C.; Dauter, Z.; Hubbard, R. E.; Bonn, T.; Engstrom, O.; Ohman, L.; Greene, G. L.; Gustafsson, J. A.; Carlquist, M. Molecular basis of agonism and antagonism in the oestrogen receptor. *Nature* **1997**, *389*, 753–758.
- (15) Shiau, A. K.; Barstad, D.; Loria, P. M.; Cheng, L.; Kushner, P. J.; Agard, D. A.; Greene, G. L. The structural basis of estrogen receptor/coactivator recognition and the antagonism of this interaction by tamoxifen. *Cell* **1998**, *95*, 927–937.
- (16) Shiau, A. K.; Barstad, D.; Radek, J. T.; Meyers, M. J.; Nettles, K. W.; Katzenellenbogen, B. S.; Katzenellenbogen, J. A.; Agard, D. A.; Greene, G. L. Structural characterization of a subtype-selective ligand reveals a novel mode of estrogen receptor antagonism. *Nat. Struct. Biol.* **2002**, *9*, 359–364.
- (17) Singh, S. M.; Gauthier, S.; Labrie, F. Androgen receptor antagonists (antiandrogens): structure-activity relationships. *Curr. Med. Chem.* **2000**, *7*, 211–247.
- (18) Souque, A.; Fagart, J.; Couette, B.; Davioud, E.; Sobrio, F.; Marquet, A.; Rafestin-Oblin, M. E. The mineralocorticoid activity of progesterone derivatives depends on the nature of the C18 substituent. *Endocrinology* **1995**, *136*, 5651–5658.
- (19) Honer, C.; Nam, K.; Fink, C.; Marshall, P.; Ksander, G.; Chatelain, R. E.; Cornell, W.; Steele, R.; Schweitzer, R.; Schumacher, C. Glucocorticoid receptor antagonism by cyproterone acetate and RU486. *Mol. Pharmacol.* **2003**, *63*, 1012–1020.
- (20) Weeks, C. M.; Duax, W. L.; Wolf, M. E. Comparison of the molecular structures of six corticosteroids. *J. Am. Chem. Soc.* **1976**, *98*, 2865–2868.
- (21) Vicent, G. P.; Monteserin, M. C.; Veleiro, A. S.; Burton, G.; Lantos, C. P.; Galigniana, M. D. 21-Hydroxy-6,19-oxidoprogesterone: a novel synthetic steroid with specific antiglucocorticoid properties in the rat. *Mol. Pharmacol.* **1997**, *52*, 749–753.
- (22) Cadepond, F.; Ulmann, A.; Baulieu, E. E. RU486 (mifepristone): mechanisms of action and clinical uses. *Annu. Rev. Med.* **1997**, *48*, 129–156.
- (23) Kauppi, B.; Jakob, C.; Farnegardh, M.; Yang, J.; Ahola, H.; Alarcon, M.; Calles, K.; Engstrom, O.; Harlan, J.; Muchmore, S.; Ramqvist, A. K.; Thorell, S.; Ohman, L.; Greer, J.; Gustafsson, J. A.; Carlstedt-Duke, J.; Carlquist, M. The three-dimensional structures of antagonistic and agonistic forms of the glucocorticoid receptor ligand-binding domain: RU-486 induces a transconformation that leads to active antagonism. *J. Biol. Chem.* **2003**, *278*, 22748–54.
- (24) Patel, F. A.; Funder, J. W.; Challis, J. R. Mechanism of cortisol/progesterone antagonism in the regulation of 15-hydroxyprostaglandin dehydrogenase activity and messenger ribonucleic acid levels in human chorion and placental trophoblast cells at term. *J. Clin. Endocrinol. Metab.* **2003**, *88*, 2922–33.
- (25) Hillisch, A.; von Langen, J.; Menzenbach, B.; Droscher, P.; Kaufmann, G.; Schneider, B.; Elger, W. The significance of the 20-carbonyl group of progesterone in steroid receptor binding: a molecular dynamics and structure-based ligand design study. *Steroids* **2003**, *68*, 869–878.
- (26) von Langen, J.; Fritzeimer, K. H.; Diekmann, S.; Hillisch, A. Molecular basis of the interaction specificity between the human glucocorticoid receptor and its endogenous steroid ligand cortisol. *ChemBioChem* **2005**, *6*, 1110–1118.
- (27) Williams, S. P.; Sigler, P. B. Atomic structure of progesterone complexed with its receptor. *Nature* **1998**, *393*, 392–396.
- (28) Bourguet, W.; Ruff, M.; Chambon, P.; Gronemeyer, H.; Moras, D. Crystal structure of the ligand-binding domain of the human nuclear receptor RXR- $\alpha$ . *Nature* **1995**, *375*, 377–382.
- (29) Horwitz, K. B.; Zava, D. T.; Thilagar, A. K.; Jensen, E. M.; McGuire, W. L. Steroid receptor analyses of nine human breast cancer cell lines. *Cancer Res.* **1978**, *38*, 2434–2437.
- (30) Beato, M. H.; Schütz, P. G. Steroid hormone receptors: Many Actors in search of a plot. *Cell* **1995**, *83*, 851–857.
- (31) Burton, G.; Lantos, C. P.; Veleiro, A. S. Method for the preparation of 21-hydroxy-6,19-oxidoprogesterone (21OH-6OP). U.S. Patent 7,071,328, 2006.
- (32) Veleiro, A. S.; Pecci, A.; Monteserin, M. C.; Baggio, R.; Garland, M. T.; Lantos, C. P.; Burton, G. 6,19-Sulfur-bridged progesterone analogues with antiimmunosuppressive activity. *J. Med. Chem.* **2005**, *48*, 5675–5683.
- (33) Gaussian 03, Revision B.05: Frisch, M. J.; Trucks, G. W.; Schlegel, H. B.; Scuseria, G. E.; Robb, M. A.; Cheeseman, J. R.; Montgomery, J. A., Jr.; Vreven, T.; Kudin, K. N.; Burant, J. C.; Millam, J. M.; Iyengar, S. S.; Tomasi, J.; Barone, V.; Mennucci, B.; Cossi, M.; Scalmani, G.; Rega, N.; Petersson, G. A.; Nakatsuji, H.; Hada, M.; Ehara, M.; Toyota, K.; Fukuda, R.; Hasegawa, J.; Ishida, M.; Nakajima, T.; Honda, Y.; Kitao, O.; Nakai, H.; Klene, M.; Li, X.; Knox, J. E.; Hratchian, H. P.; Cross, J. B.; Adamo, C.; Jaramillo, J.; Gomperts, R.; Stratmann, R. E.; Yazyev, O.; Austin, A. J.; Cammi, R.; Pomelli, C.; Ochterski, J. W.; Ayala, P. Y.; Morokuma, K.; Voth, G. A.; Salvador, P.; Dannenberg, J. J.; Zakrzewski, V. G.; Dapprich, S.; Daniels, A. D.; Strain, M. C.; Farkas, O.; Malick, D. K.; Rabuck, A. D.; Raghavachari, K.; Foresman, J. B.; Ortiz, J. V.; Cui, Q.; Baboul, A. G.; Clifford, S.; Cioslowski, J.; Stefanov, B. B.; Liu, G.; Liashenko, A.; Piskorz, P.; Komaromi, I.; Martin, R. L.; Fox, D. J.; Keith, T.; Al-Laham, M. A.; Peng, C. Y.; Nanayakkara, A.; Challacombe, M.; Gill, P. M. W.; Johnson, B.; Chen, W.; Wong, M. W.; Gonzalez, C.; Pople, J. A. Gaussian, Inc., Pittsburgh, PA, 2003.
- (34) Pearlman, D. A.; Case, D. A.; Caldwell, J. W.; Ross, W. S.; Cheatham III, T. E.; DeBolt, S.; Ferguson, D.; Seibel, G.; Kollman, P. AMBER, a package of computer programs for applying molecular mechanics, normal mode analysis, molecular dynamics and free energy calculations to simulate the structural and energetic properties of molecules. *Comput. Phys. Commun.* **1995**, *91*, 1–41.
- (35) Berendsen, H. J. C.; Postma, J. P. M.; Van Gunsteren, W. F.; DiNola, A.; Haak, J. R. Molecular dynamics with coupling to an external bath. *J. Chem. Phys.* **1984**, *81*, 3684–3690.
- (36) Cheatham III, T. E.; Cieplak, P.; Kollman, P. A modified version of the Cornell et al. force field with improved sugar pucker phases and helical repeat. *Biomol. Struct. Dynam.* **1999**, *16*, 845–862.
- (37) Amadei, A.; Linssen, A. B. M.; Berendsen, H. J. C. Essential dynamics of proteins. *Proteins: Structure, Funct. Genet.* **1993**, *17*, 412–425.